V. Diagnostics of HII Regions

A. Motivations

- Primary means of studying the metallicity, SFR, density, extinction, temperature, etc. in star-forming galaxies
- For faint galaxies, emission lines may be the only aspects (beyond photometry) that are observable

B. Primer on Saha Equation and Collisional Strengths (see RadProc notes)

C. Hydrogenic Recombination Lines

- The relative strengths of the Balmer decrement (Hα/Hβ/Hγ) can be calculated theoretically
  - ◇ The line ratios are nearly independent of T and n_e
  - ◇ Therefore, they are useful for inferring reddening because they are at widely separated wavelengths
  - ◇ Furthermore, the flux of Hβ is useful for estimating other diagnostics of the HII Region
- Setup
  - ◇ Let $n_{n'\ell'}$ equal the density of atoms in the $n'\ell'$ level
  - ◇ The statistical weights of these levels are

$$g_\ell = 2\ell + 1 \tag{1}$$

$$g_n = \sum_{\ell=0}^{n-1} (2\ell + 1) = n^2 \tag{2}$$

  - ◇ Assume $\varepsilon_{n\ell}$ is independent of ℓ
  - ◇ Selection rule: $\Delta\ell = \pm 1$
- Line emissivity

$$j_{n'n} = \frac{1}{4\pi} \sum_{\ell'=0}^{n'-1} \sum_{\ell=\ell'\pm 1} n_{n'\ell'} A_{n'\ell' n\ell} h\nu_{nn'} \tag{3}$$

  - ◇ $A_{n'\ell' n\ell}$ is the spontaneous emission rate

$$A_{n'\ell' n\ell} = 4\pi^2 \nu_{nn'}^3 \left[\frac{8\pi\alpha a_0^2}{Z^2 3c^2} \right] \frac{max(\ell, \ell')}{2\ell' + 1} |P(n'\ell', n\ell)|^2 \tag{4}$$

$$P = \int_0^\infty R_{n'\ell'}(r) r R_{n\ell}(r) dr \tag{5}$$

  - ◇ $R = r\Psi$ is the normalized radial function

- ◇ See Condon & Shortley or my AY204b notes for more

- Oscillator strength $f_{n\ell n'\ell'}$

$$A_{n'\ell' n\ell} = K_K \varepsilon_{nn'}^2 \frac{2\ell+1}{2\ell'+1} f_{n\ell n'\ell'} \tag{6}$$

$$\varepsilon_{nn'} = \frac{1}{n^2} - \frac{1}{n'^2} \tag{7}$$

$$K_K = \frac{1}{2}\frac{\alpha^5 mc^2}{\hbar} = 8.03 \times 10^9 \ \ \mathrm{s}^{-1} \tag{8}$$

- ◇ The f-values are often tabulated
- ◇ Or emperically determined
- ◇ A values are also tabulated in Wiese et al., NBS 1966

- Total decay rate from state $n\ell$

$$A_{n\ell} = \sum_{n''=n_0}^{n-1} \sum_{\ell''=\ell\pm1} A_{n\ell n''\ell''} \tag{9}$$

(a) Case A ($n_0 = 1$): This presumes all line transitions produced in the HII region escape. It is a good assumption for low mass HII regions but these are rare or, at the least, difficult to study.

(b) Case B ($n_0 = 2$): Assume all Lyman lines higher than Lyα are trapped and ultimately converted to Lyα and other lines.

- ◇ Reality generally lies between the two cases
- ◇ Lyman line cross-section (center of the line; we will derive this later)

$$\sigma(\mathrm{Ly}n) = \frac{3\lambda_{n1}^3}{8\pi}\left(\frac{m_H}{2\pi kT}\right)^{\frac{1}{2}} A_{nP,1S} \tag{10}$$

  - ▲ At $T \approx 10000\,\mathrm{K}$, $\tau(Ly\alpha) \approx 10^4$
  - ▲ Similarly, $\tau(Ly\beta) \approx 10^3, \tau(L8) \approx 10^2, \tau(L18) \approx 10$
  - ▲ The majority of interactions are scatterings
  - ▲ Occasionally, however, the photon is converted to Hα, Hβ, etc.

- Cascade Matrix
  - ◇ Means of calculating the population of various levels
  - ◇ Consider steady state conditions (i.e. detailed balancing)
    - ▲ Ignoring g_ℓ

$$n_e n_p \alpha_{n\ell}(T) + \sum_{n'>n;\ell'=\ell\pm1} n_{n'\ell'} A_{n'\ell' n\ell} = n_{n\ell} A_{n\ell} \tag{11}$$

    - ▲ Averaging over ℓ

$$n_e n_p \alpha_n + \sum_{n'=n+1}^{\infty} n_{n'} A_{n'n} = n_n A_n \tag{12}$$

▲ Definitions

$$\alpha_n = \sum_\ell \alpha_{n\ell} \tag{13}$$

$$A_{n'n} = \sum_\ell \sum_{\ell'=\ell\pm1} \frac{g_\ell}{(n')^2} A_{n'\ell' n\ell} \tag{14}$$

$$A_n = \sum_{n''=n_0}^{n-1} A_{nn''} \tag{15}$$

▲ This assumes the population of ℓ-levels is proportional to g_ℓ

▲ This is a good approximation for high n and ℓ where both e^- and p collisions give $n\ell \to n, \ell \pm 1$

◇ Define $P_{n'n}$ = probability that every entry into n' is followed by a direct transition to $n < n'$

$$P_{n'n} = \frac{A_{n'n}}{A_n} \qquad \text{(branching ratio)} \tag{16}$$

◇ Define $C_{n'n}$ = probability that entry into n' is followed by a transition to $n < n'$ by any route.

$$C_{n,n} = 1 \tag{17}$$

$$C_{n+1,n} = P_{n+1,n} \tag{18}$$

$$C_{n+2,n} = P_{n+2,n+1} C_{n+1,n} + P_{n+2,n} \tag{19}$$

$$\vdots \tag{20}$$

◇ Altogether

$$C_{n'n} = \sum_{p=n'-1}^{n} P_{n'p} C_{pn} \tag{21}$$

◇ Our equation for detailed balance becomes

$$n_n A_n = n_e n_p \sum_{n'=n}^{\infty} \alpha_{n'} C_{n'n} \tag{22}$$

▲ One generally express the solution in terms of the 'departure coefficient'

$$b_n \equiv \frac{n_n}{n_n^*} \tag{23}$$

○ n_n^* is given by the Boltzman equation (i.e. thermodynamic equilibrium)

○ Using the Boltzman-Saha equation

$$b_n = \left(\frac{2\pi m k T}{h^3} \right)^{\frac{3}{2}} \frac{e^{-I_n/kT}}{n^2 A_n} \sum_{n'=n}^{\infty} \alpha_{n'} C_{n'n} \tag{24}$$

- ∘ Note, there is no density dependence in the above equation
- ◇ An approximate solution to the Cascade matrix comes from Seaton
  - ▲ He noted $C_{gn} \to C_{\infty n}$ as $g \to \infty$
  - ▲ He replaced the higher order terms of the sum by an integral

$$\sum_{n'=n}^{\infty} \alpha_{n'} C_{n'n} = \sum_{n'=n}^{g-1} \alpha_{n'} C_{n'n} + \frac{1}{2}\alpha_g C_{gn} + \frac{1}{2}\left(C_{gn} + C_{\infty n} \right) \int_{g}^{\infty} \alpha_{n'} d_{n'} \tag{25}$$

- ◇ Given these results, the emissivity becomes

$$j_{n'n} = n_{n'} A_{n'n} h\nu_{n'n}/4\pi \tag{26}$$
$$= b_{n'} n^*_{n'} A_{n'n} h\nu_{n'n}/4\pi \tag{27}$$

- ◇ Table

Table 1: Seaton's Results (modern values)

$j_{n'n}$	Case A $T = 10^4$	$T = 2 \times 10^4$	Case B $T = 10^4$	$T = 2 \times 10^4$
Hα	191	199	271 (286)	279
Hβ	100	100	100 (100)	100
Hγ	58.9	56.9	50.6 (47)	49.1
H10	10.4	9.2	7.1 (5.4)	6.3
H20	1.6	1.4	1.0 (1.6)	0.8

  - ▲ Case B values of Hα are much higher due to the trapping of Lyman lines
  - ▲ Values in () are from Osterbrock (i.e. modern values)
  - ▲ Note that all of the lines weaken together as $T \uparrow$ ($\alpha_n \propto T^{-1/2}$ to $T^{-3/2}$)
- • More accurate Balmer decrements
  - ◇ Treat ℓ explicitly
  - ◇ Include collisional terms

$$n_e n_p \alpha_{n\ell}(T) + \sum_{n'=n+1}^{\infty} \sum_{\ell'=\ell\pm1} A_{n'\ell' n\ell} n_{n'\ell'} + \sum_{\ell'=\ell\pm1} n_e n_{n\ell'} q_{n\ell' n\ell} + \sum_{n'=n_0}^{\infty} \sum_{\ell'=\ell\pm1} n_e n_{n'\ell'} q_{n'\ell' n\ell}$$
$$= n_{n\ell} \left[A_{n\ell} + \sum_{\ell'=\ell\pm1} n_e q_{n\ell n\ell'} + \sum_{n=n_0}^{\infty} \sum_{\ell'=\ell\pm1} n_e q_{n\ell n'\ell'} \right]$$

  - ▲ $\alpha_{n\ell}(T)$ are determined using Milne's relation
  - ▲ Define

$$A_{n\ell} = \sum_{n''=n_0}^{n-1} \sum_{\ell''=\ell\pm1} A_{n\ell n''\ell''} \tag{28}$$

- ▲ Collisions
  - ○ $q_{n\ell \to n\ell \pm 1}$ collisions are due to impacts by ions (Pengalley & Seaton 1964)
  - ○ $q_{n\ell \to n\pm 1 \ell \pm 1}$ collisions are due to electrons (Seraph 1964)
- ▲ See Osterbrock Tables 4.1 to 4.4

D. Effective Recombination Coefficient for Hβ: $\alpha_{H\beta}$

- Fig

- Define

$$\alpha_{H\beta} = \alpha_B P_{H\beta} \tag{29}$$

- ◇ $P_{H\beta}$ is the probability of Hβ emission following recombination to higher excited levels
- ◇ Ignoring collisions

$$P_{H\beta} = \sum_{n'=4}^{\infty} \sum_{\ell'=0}^{n'-1} \alpha_{n'\ell'} \sum_{\ell'=\ell\pm 1} C_{n'\ell' n\ell} \sum_{\ell''=\ell\pm 1} \frac{A_{4\ell,2\ell''}}{A_{4\ell}} \tag{30}$$

$$\approx 0.11 \tag{31}$$

- ◇ From Brocklehurst ($\varepsilon_{H\beta} \equiv \alpha_{H\beta} h\nu_{H\beta}$):

Table 2: Hβ RECOMBINATION COEFFICIENT

T	$\alpha_{H\beta}$ (cm^3/s)	$\varepsilon_{H\beta}$ (erg cm^3 / s)
0.5×10^4	5.4×10^{-14}	2.2×10^{-25}
1.0×10^4	3.0×10^{-14}	1.24×10^{-25}
2.0×10^4	1.6×10^{-14}	6.5×10^{-26}

- ◇ Functional fit

$$\alpha_{H\beta} h\nu_{H\beta} \approx 1.24 \times 10^{-25} \left(\frac{T}{10^4 \mathrm{K}} \right)^{-0.8795} \quad (\mathrm{erg\,cm^3/s}) \tag{32}$$

- Diagnostic of n_e or M_{HII}
  - ◇ Measure $F_{H\beta}$

$$L_{H\beta} \approx F_{H\beta} 4\pi d^2 = \varepsilon_{H\beta} \frac{4}{3} \pi R^3 n_e^2 \tag{33}$$

  - ◇ If R/d is known, n_e can be estimated
  - ◇ If n_e is known (e.g. [OII]), then M_{HII} is inferred

$$M_{HII} \approx \frac{F_{H\beta} 4\pi d^2 m_p}{\varepsilon_{H\beta} n_e} \tag{34}$$

- Zanstra's Method for finding T_* of the ionizing star (or the ionizing luminosity, ϕ) in an HII region
  (a) Observe the size of the HII region r_{HII}. Global ionization equilibrium (e.g. the Stromgren radius) implies:

$$\phi = \int_0^{r_{HII}} \alpha_B n_e^2 4\pi r^2 dr \tag{35}$$

  - ◇ For an ionization bounded HII region, $r_{HII} = R_S$
  - ◇ For $r_{HII} < R_S$, this is a density bounded region and ϕ is greater than the RHS of Equation 35.

  (b) Observe $F_{H\beta}$

$$F_{H\beta} = \frac{1}{4\pi d^2} \left\{ h\nu_{H\beta} \int_0^{r_{HII}} \alpha_{H\beta} n_e^2 4\pi r^2 dr \right\} \tag{36}$$

  - ◇ If the nebula is nearly isothermal, then $\alpha_{H\beta}$ = constant and α_B = constant with radius
  - ◇ In this case, the integral is trivial

  (c) Rearranging

$$\phi \geq \frac{4\pi d^2 F_{H\beta}}{h\nu_{H\beta}} \left(\frac{\alpha_B}{\alpha_{H\beta}} \right) \tag{37}$$

  (d) For a star (blackbody)

$$\phi(T_*) = \frac{15}{\pi^4} \frac{L}{h\nu_0} f\left(\frac{h\nu_0}{kT_*} \right) \quad \mathrm{s}^{-1} \tag{38}$$

  - ◇ $L = 4\pi R_*^2 \sigma T_*^4$
  - ◇ Note, ϕ is a double-valued function of T_*

  (e) If the visible (V-band) flux is also known

$$F_V = \frac{4\pi R_*^2}{4\pi d^2} \int_0^\infty \pi B_\nu(T_*) V_\nu d\nu \tag{39}$$

$$= \frac{L}{\sigma T_*^4} \frac{1}{4\pi d^2} \int_0^\infty \pi B_\nu V_\nu d\nu \tag{40}$$

- ◇ V_ν is the V-band filter

(f) Rearrange the 3rd step

$$F_{H\beta} \leq \frac{\alpha_{H\beta}}{\alpha_B} \frac{h\nu_{H\beta}\phi}{4\pi d^2} = \frac{\alpha_{H\beta}}{\alpha_B} \frac{h\nu_{H\beta}}{4\pi d^2} \frac{15}{\pi^4} \frac{L}{h\nu_0} f \tag{41}$$

(g) Divide step 5 by 6

$$\frac{F_{H\beta}}{F_V} \leq \frac{\alpha_{H\beta}}{\alpha_B} h\nu_{H\beta} \frac{15}{\pi^4} \frac{f}{h\nu_0} \frac{\sigma T_*^4}{\int\limits_0^\infty \pi B_\nu(T_*) V_\nu d\nu} \tag{42}$$

- ◇ Gives a known function of T and T_*
- ◇ Solve for T_*, independent of L and d

E. Forbidden Lines (Densty, Temperature)

- These states are generally excited by collisions
  - ◇ Gas is optically thin to forbidden lines (no radiative transfer)
  - ◇ Excited levels of forbidden lines are populated by collisions $\Rightarrow$ sensitive to n_e or T
  - ◇ Important diagnostics of density and temperature
  - ◇ e.g. [OIII], [OII]
- [OIII]
  - ◇ Configuration: $1s^2 2s^2 2p^2$
  - ◇ Two equivalent p electrons
    - ▲ Allowed states: $^1S_0; {}^3P_{0,1,2}; {}^1D_2$
    - ▲ Other states are excluded by Pauli
  - ◇ Relative energies: Hund's Rules (See RadProc notes)
    (a) Higher $S \Rightarrow$ Lower energy
    ^3P_J has lowest energy
    (b) Higher $L \Rightarrow$ Lower energy
    $^1D_2$ has lower energy than $^1S_0$
    (c) Higher $J \Rightarrow$ Higher energy for less than half filled
    $^3P_0$ has lower energy than $^3P_1$, etc.
  - ◇ Energy level diagram

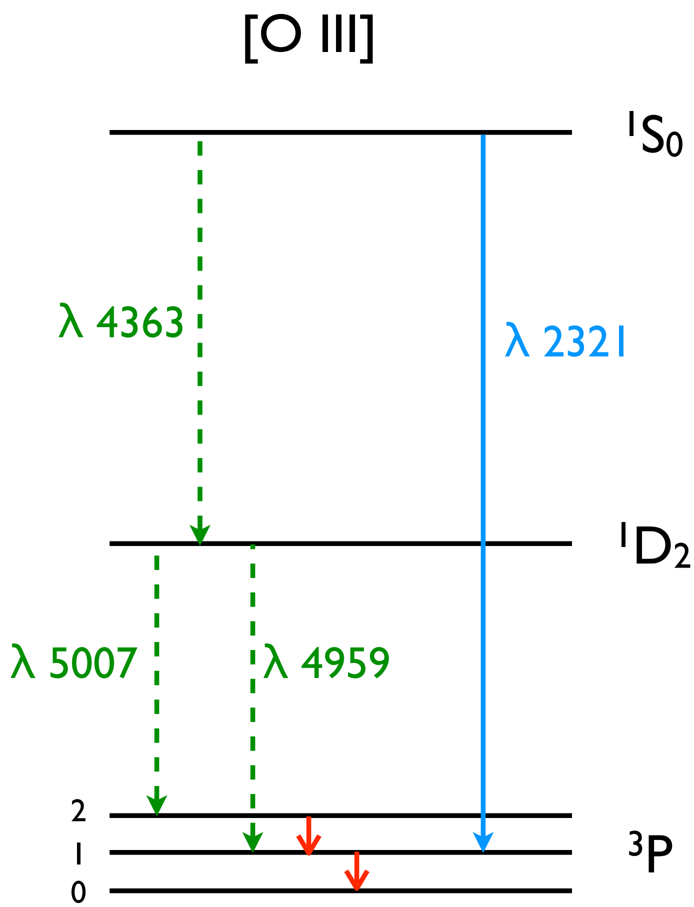

- ◇ Wavelengths
  $^1S_0 \rightarrow {}^1D_2 \quad \lambda = 4363\text{Å}$
  $^1D_2 \rightarrow {}^3P_2 \quad \lambda = 5007\text{Å}$
  $^1D_2 \rightarrow {}^3P_1 \quad \lambda = 4959\text{Å}$
  $^1D_2 \rightarrow {}^3P_0 \quad \lambda = 4931\text{Å}$
- ◇ Transitions between any two of these states is forbidden
  - ▲ No change in parity
  - ▲ Parity of two p electrons is always even

- [OIII]: Temperature diagnostic
  - ◇ Low density limit ($n_e < 10^5\,\text{cm}^{-3}$)
  - ◇ The low lying ^3P states have very nearly the same energy and are populated according to their statistical weights $g_J = (2J+1)$
  - ◇ Keys:
    - ▲ Relative excitation of the upper levels is a function of T and not n_e
    - ▲ Every excitation is followed by spontaneous emission of a photon
  - ◇ Excitation of ^1D level
    - ▲ Followed by emission of λ_{5007} or λ_{4959} photon
    - ▲ Relative probabilities $\rightarrow A_{^1D,^3P_2} : A_{^1D,^3P_1} \approx 3$

- Excitation of ^1S level
  - Emission of $\lambda_{4363}(^1D_2)$ or $\lambda_{2321}(^3P_1)$ photon
  - Relative probabilities $\rightarrow A_{^1S,^1D} : A_{^1S,^3P_1} \approx 10$
  - Emission of λ_{4363} is followed by λ_{5007} or λ_{4959} photon (small contribution)
- Emission line strength (energy/s/volume)
  - Consider $^1S \rightarrow {}^1D$

$$j_{4363} = \left[\,\text{rate } ^1S \text{ is populated}\,\right] \times \left[\,h\nu(4363)\,\right] \times \left[\,\text{rate } ^1S \rightarrow {}^1D\,\right] \tag{43}$$

    - Collisional excitation rate

$$n_{^3P}\; q_{^3P,^1S} = \frac{n_{^3P}\; 8.629 \times 10^{-6}\; \Omega(^3P,^1S)\; \mathrm{e}^{-h\nu(^1S,^3P)/kT}}{T^{\frac{1}{2}} g_{^3P}} \tag{44}$$

    - Rate $^1S \rightarrow {}^1D_2$: Ratio of spontaneous emission coefficient

$$\frac{A_{^1S,^1D}}{A_{^1S,^1D} + A_{^1S,^3P_1}} \tag{45}$$

    - Altogether

$$j_{4363} \propto \frac{n_{^3P}\Omega(^3P,^1S)\; \mathrm{e}^{-h\nu(^1S,^3P)/kT}}{T^{\frac{1}{2}} g_{^3P}}\; \frac{\nu(^1S,\,^1D)A_{^1S,^1D}}{A_{^1S,^1D} + A_{^1S,^3P_1}} \tag{46}$$

  - Consider $^1D \rightarrow {}^3P$
    - Convenient to consider the two channels together

$$j_{4959} + j_{5007} \propto \frac{n_{^3P}\Omega(^3P,\,^1D)\; \mathrm{e}^{-h\nu(^1D,^3P)/kT}}{T^{\frac{1}{2}} g_{^3P}}\; \bar{\nu}(^1D,^3P) \tag{47}$$

    - where

$$\bar{\nu}(^1D,^3P) = \frac{\nu(^1D,^3P_2)A_{^1D,^3P_2} + \nu(^1D,^3P_1)A_{^1D,^3P_1}}{A_{^1D,^3P_2} + A_{^1D,^3P_1}} \tag{48}$$

    - For higher accuracy, we should include the contribution of de-excitations from the $^1S \rightarrow {}^1D$ transition
    - But, these are small for $T < 30000$K
- Emission-line ratio

$$\frac{j_{4959} + j_{5007}}{j_{4363}} = \frac{\Omega(^3P,^1D)}{\Omega(^3P,^1S)}\,\frac{A_{^1S,^1D} + A_{^1S,^3P}}{A_{^1S,^1D}}\,\frac{\bar{\nu}(^3P,^1D)}{\nu(^1S,^1D)}\mathrm{e}^{\Delta E/kT} \tag{49}$$

  - $\Delta E = h\nu(^1S,^1D)$
  - The only physical dependence of the line ratio is temperature
  - Excellent T diagnostic for low density regimes
  - At higher n_e, collisional de-excitation is important and ^1D is preferentially weakened.

▲ Can correct equation (49) by a factor

$$f = \text{[See AGN2]} \tag{50}$$

◇ Useful expression (not quite exact)

$$\frac{j_{4959} + j_{5007}}{j_{4363}} = \frac{6.91 \times \exp\left[\,(2.5 \times 10^4)/T\,\right]}{1 + 2.5 \times 10^{-3}(n_e/T^{\frac{1}{2}})} \tag{51}$$

◇ A similar relation holds for [NII] lines, but these lines are less luminous than oxygen

◇ Since [OIII] is a major coolant of HII regions, we expect higher temperatures when the O abundance is lower.

▲ Indeed, T_e is observed to increase with the distance from the center of the Galaxy

▲ Fig (Shaver et al. 1983)

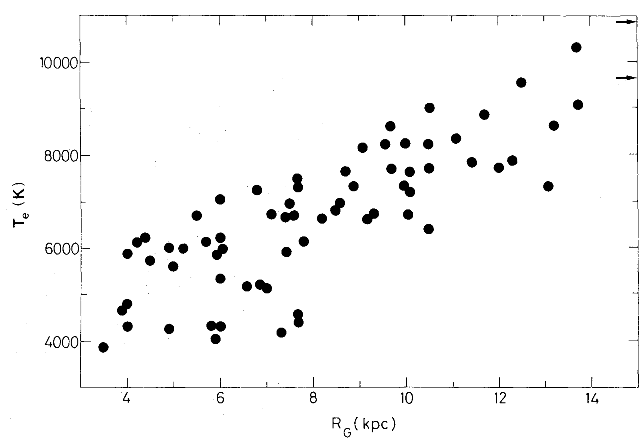

Figure 16. Electron temperatures plotted against galactocentric radius. The horizontal arrows at the upper right represent N 66 and 30 Doradus in the Magellanic Clouds.

• [OII] Configuration

◇ Ground state: $1s^2 2s^2 2p^3$

◇ Three equivalent p electrons

▲ Add 1 equivalent p electron to the $2p^2$ states

▲ Allowed states: ${}^4S_{\frac{3}{2}}; {}^2P_{\frac{1}{2},\frac{3}{2}}; {}^2D_{\frac{3}{2},\frac{5}{2}}$

◇ Relative energies: Hund's Rules

(a) Higher $S \Rightarrow$ Lower energy
${}^4S_{\frac{3}{2}}$ has lowest energy

(b) Higher $L \Rightarrow$ Lower energy
${}^2D_{\frac{3}{2},\frac{5}{2}}$ are second

(c) Half full $\Rightarrow$ All bets are off ${}^2P_{\frac{1}{2}}$ is higher than ${}^3P_{\frac{3}{2}}$
${}^2D_{\frac{3}{2}}$ is higher than ${}^2D_{\frac{5}{2}}$

- Wavelengths
  ${}^2D_{\frac{3}{2}} \rightarrow {}^4S_{\frac{3}{2}} \quad \lambda = 3726\text{Å}$
  ${}^2D_{\frac{5}{2}} \rightarrow {}^4S_{\frac{3}{2}} \quad \lambda = 3729\text{Å}$
- Energy level diagram

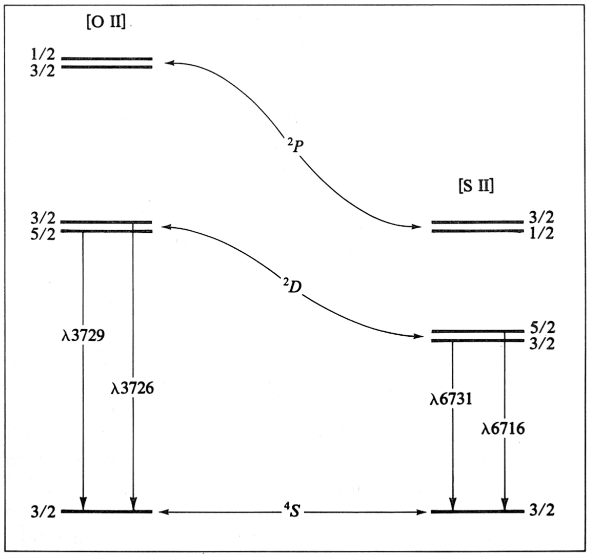

FIGURE 5.2
Energy-level diagrams of the $2p^3$ ground configuration of [O II] and $3p^3$ ground configuration of [S II].

- Transitions between any two of these states is forbidden
  - No change in parity
  - Parity of three p electrons is always odd

- [OII]: Density diagnostic
  - Pair of emission lines with very nearly the same energy
    - $\Rightarrow \; e^{\Delta E/kT} \approx 1$
    - No significant T dependence, only n_e
  - Low density limit: Every collisional excitation is followed by a spontaneous emission

$$\frac{j_{3729}}{j_{3726}} \propto \frac{\Omega(^4S,^2D_{\frac{5}{2}})\;\nu(^4S,^2D_{\frac{5}{2}})}{\Omega(^4S,^2D_{\frac{3}{2}})\;\nu(^4S,^2D_{\frac{3}{2}})} e^{-\Delta E/kT} \tag{52}$$

    - $\Delta E \ll kT$ for reasonable $T \Rightarrow e^{-\Delta E/kT} \approx 1$
    - $\nu(^4S,^2D_{\frac{5}{2}})/\nu(^4S,^2D_{\frac{3}{2}}) \approx 1$
    - Useful relation:

$$\Omega(S'L'J', SLJ) = \frac{(2J+1)}{(2S+1)(2L+1)}\,\Omega(S'L', SL) \tag{53}$$

    - Therefore

$$\Omega(^4S,^2D_{\frac{5}{2}}) = \frac{3}{2}\Omega(^4S,^2D_{\frac{3}{2}}) \tag{54}$$

▲ And

$$\frac{j_{3729}}{j_{3726}} \propto 1.5 \qquad (n_e \ll 10^3\,\mathrm{cm}^{-3}) \tag{55}$$

◇ High density limit: Levels are Boltzmann populated

$$\frac{j_{3729}}{j_{3726}} = \frac{g_{3729}}{g_{3726}} \frac{A_{3729}}{A_{3726}} = 0.3 \tag{56}$$

◇ Transition between these two regimes occurs at the critical density

$$n_e = \frac{A}{q} \approx \begin{cases} 3 \times 10^3\,\mathrm{cm}^{-3} & {}^2D_{\frac{5}{2}} \\ 1.6 \times 10^4\,\mathrm{cm}^{-3} & {}^2D_{\frac{3}{2}} \end{cases} \tag{57}$$

◇ AGN^2 Fig 5.8

- Real World
  - ◇ Often the observations of n_e and T from different forbidden lines or other methods do not always agree
    - ▲ Could be due to incorrect assumptions in the relative abundances
    - ▲ More likely, the problem is that there are variations in the temperature that are not considered in 'one-zone' models
  - ◇ Piembert fluctuation method

F. Metallicity

- Definition and Notation
  - ◇ Fraction of a gas/star/galaxy (by number or mass) that is made of metals
    - ▲ Often assessed with a single element (e.g. O, Fe, C)
    - ▲ And scaled against the Sun
  - ◇ HII formalism: 12 + log (O/H)
    - ▲ O/H is the number density of the particles
    - ▲ $(\mathrm{O/H})_\odot \approx 10^{-3.4}$, but this keeps changing!
  - ◇ 'Square-bracket' notation: $[\mathrm{O/H}] = \log(\mathrm{O/H}) - \log(\mathrm{O/H})_\odot$
    - ▲ Stellar dominated
    - ▲ IGM, ISM
- Observations
  - ◇ Local HII regions: Wealth of diagnostics we have been discussing and more
  - ◇ Extragalactic: Often limited to the strongest lines observed at optical wavelengths
    - ▲ Sensitivity of detectors and sky lines limit IR observations (improving)
    - ▲ Things are progressing to the IR, however
  - ◇ Lines

- ▲ Strong: [OII], Hβ, [OIII] $\lambda 4959, 5007$, Hα, [NII]
- ▲ Weak: [OIII] $\lambda 4363$, [SII]

◇ Key systematic observational error: Reddening

- ▲ Often use Hα/Hβ ratio and Case B assumption to estimate the reddening
- ▲ One generally has to assume an extinction law

• T_e-Method

◇ Often considered the 'gold-standard' of abundance estimates

◇ Literature (Lots)

- ▲ Shaver et al. 1983, MNRAS, 204, 53
- ▲ Skillman 1998 http://nedwww.ipac.caltech.edu/level5/Skillman/frames.html
- ▲ Dopita et al. 2006, ApJS, 167, 177

◇ Basic procedure

(a) Use specific lines to estimate T_e and n_e for the HII region
(b) Construct an HII model based on these parameters
(c) Solve for the metallicity based on the line fluxes of other lines
(d) Iterate steps (a-c) as necessary

◇ Challenges

- ▲ Difficult to estimate T_e: [OIII] $\lambda 4363$ is very weak, especially in higher metallicity systems
- ▲ One must still make many simplifying assumptions about the HII region(s)
- ▲ How does one model a full galaxy of HII regions?!

◇ More advanced efforts

- ▲ Include extinction
- ▲ Include variable T_e
- ▲ Include a range of stellar temperatures or a synthesis of multiple HII regions
- ▲ Fit for all lines together

• Empirical techniques

◇ Basic approach

- ▲ Measure O/H for a set of HII regions using the T_e-method
- ▲ Search for correlations between O/H and strong emission lines
- ▲ Derive fitting formulas and proceed

◇ R_{23} method :: Historical favorite

- ▲ Pagel et al. 1979, MNRAS, 189, 95
- ▲ Definition

$$R_{23} = \frac{I_{[\mathrm{OII}]\,\lambda\, 3727+3729} + I_{[\mathrm{OIII}]\lambda 4259+\lambda 5009}}{I_{\mathrm{H}\beta}} \tag{58}$$

▲ Empirical result (Pilyugin 2000, A& A, 362, 325)

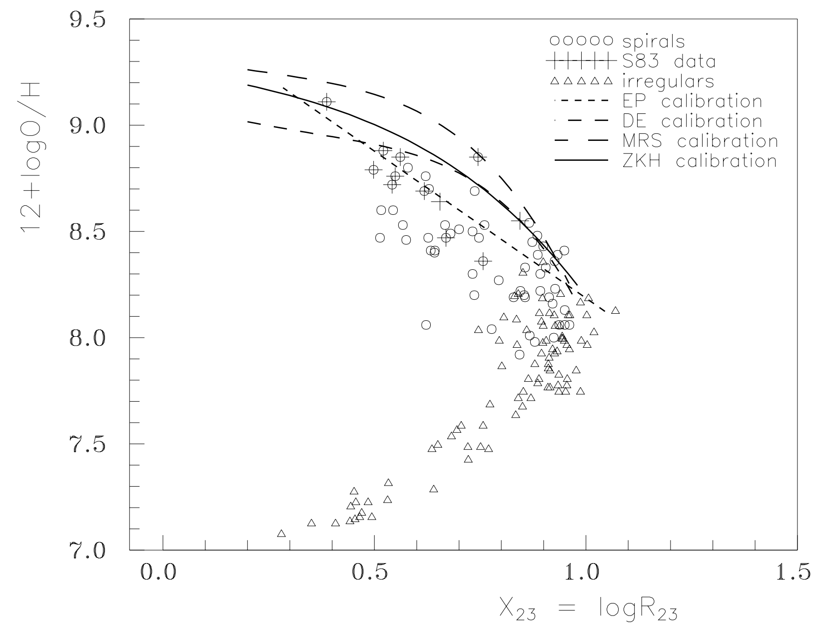

Fig. 1. The OH – logR_{23} diagram. The positions of H II regions in spiral galaxies (circles) (the H II regions in our Galaxy from Shaver et al. 1983 (S83) are indicated by plusses) and in irregular galaxies (triangles) are shown together with OH – R_{23} calibrations of different authors: Edmunds & Pagel 1984 (EP), McCall et al. 1985 (MRS), Dopita & Evans 1986 (DE), and Zaritsky et al. 1994 (ZKH).

◦ Note: The results are double-valued!!!

◦ One must have additional knowledge to break the degeneracy

▲ Functional form for low metallicity

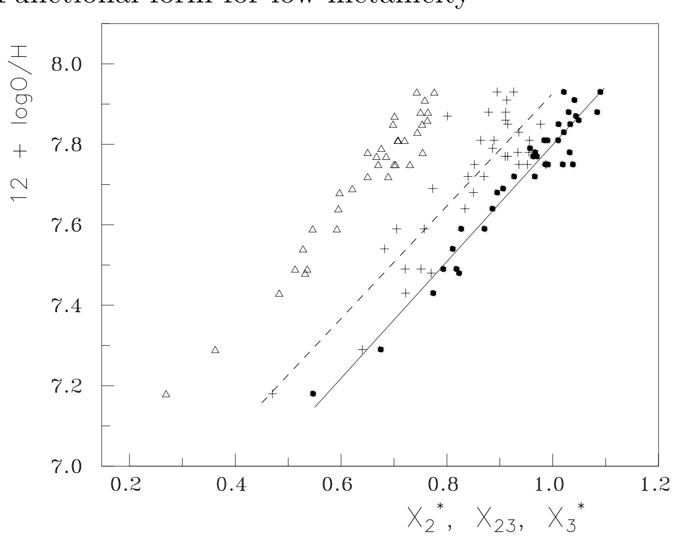

Fig. 4. The oxygen abundances (O/H)$_{Te}$ versus observed X$_{23}$ and

$$12 + \log(\mathrm{O/H})_{R23} = 6.53 + 1.40 \log R_{23} \qquad (59)$$

▲ Functional form for high metallicity

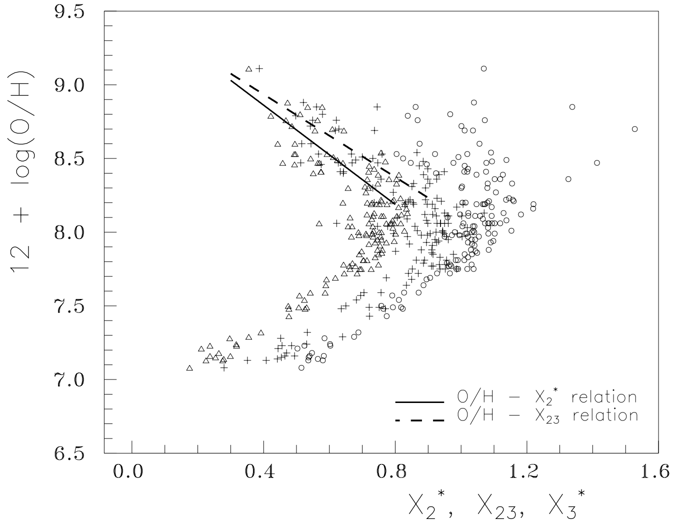

Fig. 8. The oxygen abundances (O/H)$_{Te}$ versus observed X$_{23}$ (plusses)

$$12 + \log(\mathrm{O/H})_{R23} = 9.50 - 1.40 \log R_{23} \tag{60}$$

◇ [NII], Hα, [OIII] methods

- ▲ Literature
  - ∘ Alloin et al. 1979, A& A 78, 200
  - ∘ Pettini & Pagel 2004, MNRAS, 348, L59
- ▲ Motivations
  - ∘ Break the R_{23} degeneracy
  - ∘ Still simpler than the T_e method
  - ∘ Push to higher z
- ▲ N2 index
  - ∘ Definition

$$N2 = \log([\mathrm{NII}]\lambda6583/\mathrm{H}\alpha) \tag{61}$$

  - ∘ Empirical

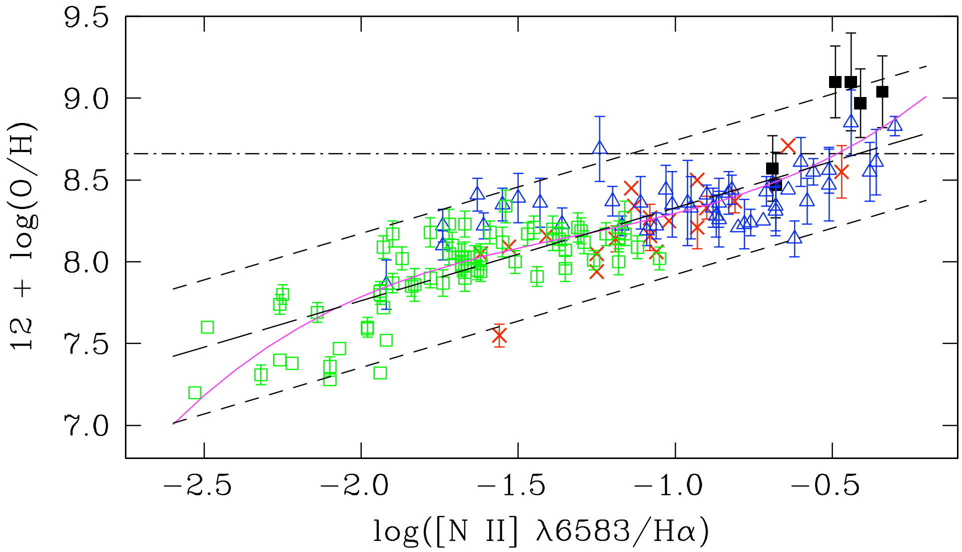

- Relation

$$12 + \log(\mathrm{O/H}) = 8.90 + 0.57 \times N2 \tag{62}$$

▲ O3N2 index

- Definition

$$O3N2 = \log\{\,([\mathrm{OIII}]\lambda5007/\mathrm{H}\beta)/([\mathrm{NII}]\lambda6583/\mathrm{H}\alpha)\,\} \tag{63}$$

- Empirical

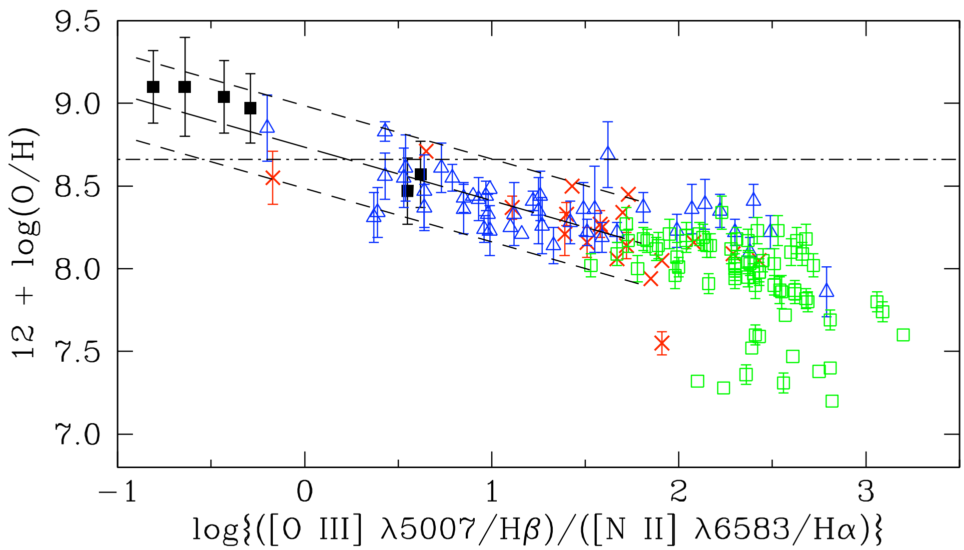

- Relation

$$12 + \log(\mathrm{O/H}) = 8.73 - 0.32 \times O3N2 \tag{64}$$

G. Star Formation Rate (SFR)

- Because HII emission lines are produced by short-lived, massive stars, their integrated intensity should scale with the star-formation rate in a galaxy

- I will leave a proper treatment/discussion of this topic to other classes.
- Allow me to point you to Kennicutt 1998, ARA& A, 36, 189 as a starter